

## **Supporting Information**

### **DNA-Based pH Nanosensor with Adjustable FRET Responses to Track Lysosomes and the pH Fluctuations**

Xinmin Yue<sup>†</sup>, Yanqi Qiao<sup>†</sup>, Dening Gu<sup>†</sup>, Rui Qi<sup>†</sup>, Hongjie Zhao<sup>†</sup>, Yongmei Yin<sup>†</sup>, Wei Zhao<sup>†</sup>, Rimo Xi<sup>\*†</sup>, Meng Meng<sup>\*†</sup>

<sup>†</sup> State Key Laboratory of Medicinal Chemical Biology, College of Pharmacy and KLMDASR of Tianjin, Nankai University, Tongyan Road, Haihe Education Park, Tianjin, 300350, People's Republic of China

\*Corresponding author:

Rimo Xi:

Phone: (86)-22-23506290

Fax: (86)-22-23507760

E-mail: xirimo@nankai.edu.cn

Meng Meng:

Phone: (86)-22-23506290

Fax: (86)-22-23507760

E-mail: mengmeng@nankai.edu.cn

## Table of Contents

<b>S-3. Experimental Section:</b>	Materials and reagents; Cell lines and cell culture; Image Analysis
<b>S-4.</b>	Table S1. Oligonucleotide sequences used in this paper
<b>S-5.</b>	Table S2. DNA strands used to construct the probes designed in this work
<b>S-6.</b>	Figure S1. DNA sequences and the structures of the pH-responsive probes
<b>S-7.</b>	Figure S2. Values and ratios of normalized fluorescence intensity of Cy3 and Cy5
<b>S-8.</b>	Figure S3. The fluorescence spectra of the pH-responsive probes
<b>S-9.</b>	Figure S4. Fluorescence performance of the FAM and TAMRA labelled probe
<b>S-10.</b>	Figure S5. Thermal stability of pH-i and pH-s
<b>S-11.</b>	Figure S6. Thermal stability of pH-Td
<b>S-12.</b>	Figure S7. pH stability of the structure of pH-Td
<b>S-13.</b>	Figure S8. Agarose analysis and FRET-response properties of pH-Td7nt
<b>S-14.</b>	Figure S9. Agarose analysis and FRET-response properties of pH-Td-1
<b>S-15.</b>	Figure S10. The performance of dual-labelled ATP-i to sense ATP
<b>S-16.</b>	Figure S11. The performance of dual-labelled ATP-Td to sense ATP
<b>S-17.</b>	Figure S12. The FBS-mediated degradation analysis of pH-Td, pH-i and pH-s
<b>S-18.</b>	Figure S13. The biostability evaluations of pH-Td in nucleases
<b>S-19.</b>	Figure S14. The MTT assay
<b>S-20.</b>	Figure S15. The intracellular performance of pH-i, pH-s and pH-Td
<b>S-21.</b>	Figure S16. Receptor-mediated internalization of the pH-Td
<b>S-22.</b>	Table S3. A comparison of different pH sensors
<b>S-23.</b>	Reference

## **1. Materials and reagents**

The HPLC purified DNA sequences used in this work were purchased from Sangon Biotech Co., Ltd. (Shanghai, China) (Table S1). Thiazolyl blue tetrazolium bromide (MTT) was supplied from Beyotime Biotech. Co., Ltd. (Shanghai, China). Chloroquine (CQ), ATP and nigericin were purchased from Aladdin Biochemical Technology Co., Ltd. (Shanghai, China). Lysotracker Green and Mitotracker Green were purchased from Meilunbio Co., Ltd. (Dalian, China). DNA ladder and DNase I were from TaKaRa Bio Inc. (Dalian, China). Cell lines were purchased from Gaining Biological Co., Ltd. (Shanghai, China). Dulbecco's modified Eagle's medium (DMEM), fetal bovine serum (FBS) and penicillin-streptomycin were from Biological Industries (Israel). All solutions were prepared using deionized water ( $\geq 18.2$  M $\Omega$ , Milli-Q, Millipore).

## **2. Cell lines and cell culture**

NIH 3T3 cells (embryonic mouse fibroblast) were cultured in DMEM with 10% FBS and 1% penicillin-streptomycin. Cells were cultured in a humidified atmosphere (5% CO<sub>2</sub>) at 37°C.

## **3. Image Analysis in Lysosome Imaging Experiment**

Each endosome in the merged image was selected by the ROI plugin in Image J/Fiji. The fluorescence intensities of the vesicles in the FRET image (Cy5) and the donor image (Cy3) were measured to provide a FRET ratio (Cy5/Cy3).

**Table S1.** Oligonucleotide sequences used in this work

No.	Name	Sequence (5' to 3')
(1)	L1	ACATTCCTAAGTCTGAAACATTACAGCTTGCTACACGAGAAGAGCCGCCATAGTA
(2)	L2-5A	<b>Cy5</b> -AACCCCTTTCCCCCGGTTTTTTTTTTTTTCAACTGCCTGGTGATAAA ACGACACTACGTGGGAATCTACTATGGCGGCTCTTC
(3)	L3-3A	TATCACCAGGCAGTTGACAGTGTAGCAAGCTGTAATAGATGCGAGGGTCCAATAC TTTTTTTTTTTTTTTCCCCCTTTCCCCC- <b>Cy3</b>
(4)	L4	TTCAGACTTAGGAATGTGCTTCCCACGTAGTGTCTGTTTGTATTG GACCCTCGCAT
(5)	L2-5A-1	<b>Cy5</b> -AACCCCTTTCCCCCGGTTTTTTTTTTTTTCAACTGCCTGGTGATAAAA CGACACTACGTGGGAATCTACTATGGCGGCTCTTC
(6)	L3-3A-1	TATCACCAGGCAGTTGACAGTGTAGCAAGCTGTAATAGATGCGAGGGTCCAATAC TTTTTTTTTTTTTTTCCCCCTTTCCCCC- <b>Cy3</b>
(7)	pH-i	<b>Cy5</b> -AACCCCTTTCCCCCTTTCCCCCTTTCCCCC- <b>Cy3</b>
(8)	pH-i-1	<b>Cy5</b> -AACCCCTTTCCCCCTTTCCCCCTTTCCC- <b>Cy3</b>
(9)	pH-5a	<b>Cy5</b> -AACCCCTTACCCCCCGG
(10)	pH-3a	TTCCCCATTCCCCC- <b>Cy3</b>
(11)	pH-5-1	<b>Cy5</b> -AACCCCTTTCCCCTATTTTTTTTTTTTTT
(12)	pH-3-1	AAAAAAAAAAATTCCCTTTCCCCC- <b>Cy3</b>
(13)	pH-5+1	<b>Cy5</b> -AACCCCTTTCCCCCTATTTTTTTTTTTTTT
(14)	pH-3+1	AAAAAAAAAAATTCCCTTTCCCCCC- <b>Cy3</b>
(15)	pH-A	<b>TAMRA</b> -AACCCCTTTCCCCCTATTTTTTTTTTTTTT
(16)	pH-B	AAAAAAAAAAATTCCCTTTCCCCC- <b>FAM</b>
(17)	pH-5	<b>Cy5</b> -AACCCCTTTCCCCCTATTTTTTTTTTTTTT
(18)	pH-3	AAAAAAAAAAATTCCCTTTCCCCC- <b>Cy3</b>
(19)	AT-5s	<b>Cy5</b> -ACCTGGGGGAGTAT
(20)	AT-3s	TGCGGAGGAAGGT- <b>Cy3</b>
(21)	ATP-53	<b>Cy5</b> -ACCTGGGGGAGTATTGCGGAGGAAGGT- <b>Cy3</b>
(22)	ATL2-5	<b>Cy5</b> -ACCTGGGGGAGTATTTTTTTTTTTTTTCAACTGCCTGGTGATAAAAC GACACTACGTGGGAATCTACTATGGCGGCTCTTC
(23)	ATL3-3	TATCACCAGGCAGTTGACAGTGTAGCAAGCTGTAATAGATGCGAGGGTCCAATAC TTTTTTTTTTTTTTTGCAGGAGGAAGGT- <b>Cy3</b>
(24)	7L1	GAGCGTTAGCCACACACACAGTC
(25)	7L2-5A	<b>Cy5</b> -AACCCCTTTCCCCCGGTTTTTTTTTTTTTTAGGCGAGTGTGGCAGAGGTGT
(26)	7L3-3A	CGCCTAAACAAGTGGAGACTGTGTTTTTTTTTTTTTTTCCCCCTTTCCCCC- <b>Cy3</b>
(27)	7L4	AACGCTCACCCTTGAACACCTC

In all probes, the Cy5 was used to label the 5' end, and the Cy3 was used to label the 3' end.

**Table S2.** Probes designed in this paper and the DNA strands used to construct the probe

Probe name	DNA Strands No.
pH-s-1	(11),(12)
pH-s	(17),(18)
pH-s+1	(13),(14)
pH-i-1	(8)
pH-i	(7)
pH-Td	(1),(2),(3),(4)
pH-Td7nt	(24), (25), (26), (27)
pH-ss	(9),(10)
pH-Td-1	(1),(4),(5),(6)
ATP-i	(21)
ATP-Td	(1),(4),(22),(23)

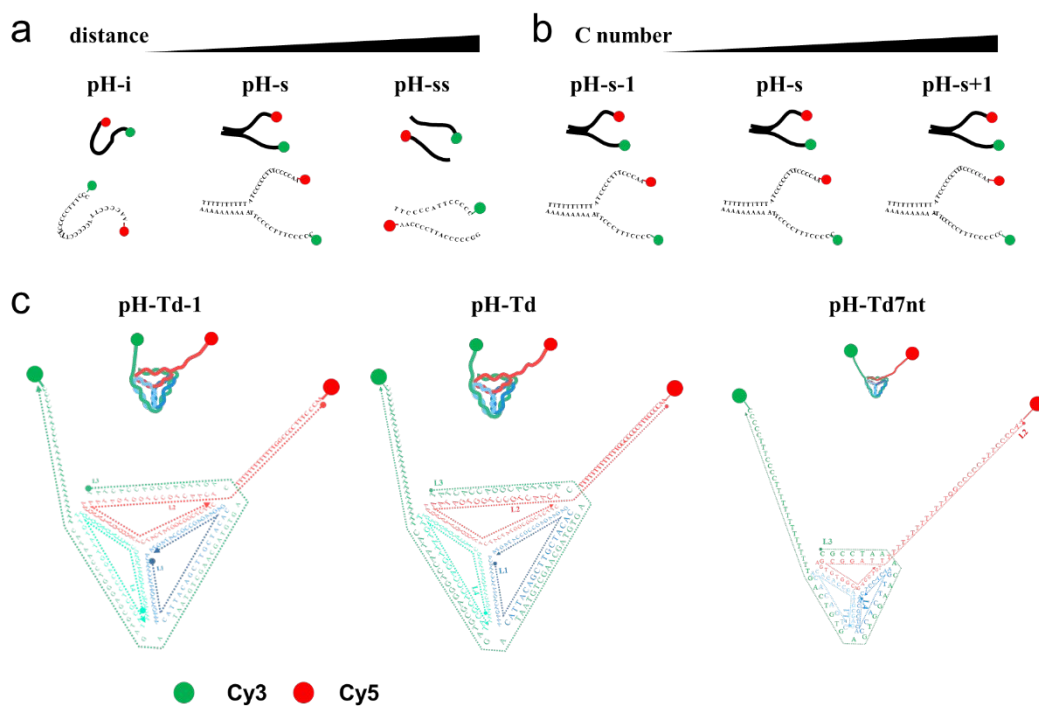


**Figure S1.** DNA sequences and the structures of the pH-responsive probes used in this work.

(a) The probes pH-i, pH-s and pH-ss were designed to study the influence of the distance between two split parts on the pH-response ability. (b) The probes pH-s-1, pH-s and pH-s+1 were designed to investigate the influence of C-tracts length on the pH sensing. (c) DNA sequences and the structures of pH-Td-1, pH-Td, pH-Td7nt.

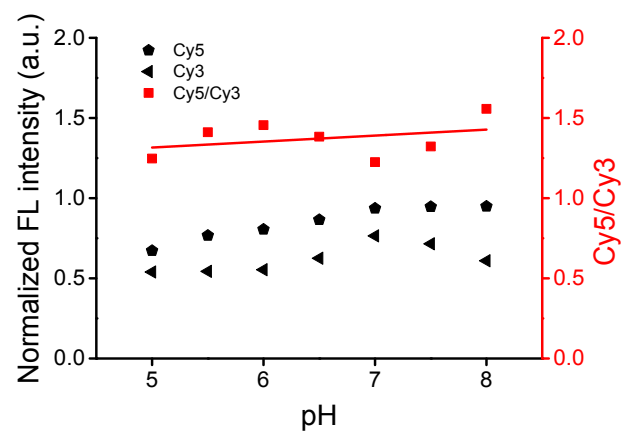


**Figure S2.** Fluorescence intensity and ratios of Cy3 at 568 nm and Cy5 at 668 nm in different pH conditions. (Sequence No. 19 used for Cy5, Sequence No. 20 used for Cy3)

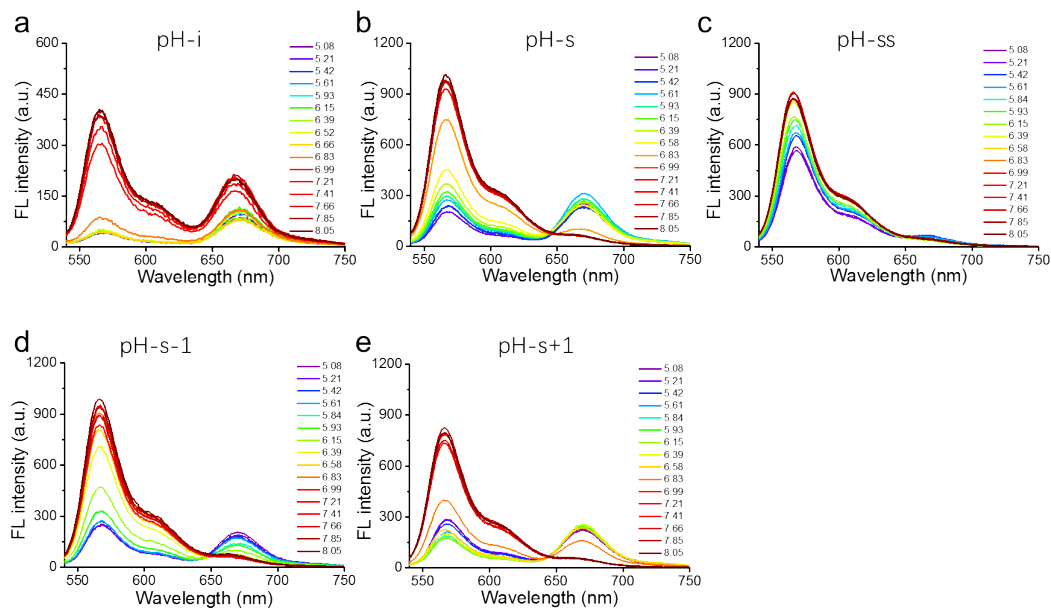


**Figure S3.** Fluorescence performance of the designed probes at different pH conditions. (a) Fluorescence emission spectra of pH-i. (b) Fluorescence emission spectra of pH-s. (c) Fluorescence emission spectra of pH-ss. (d) Fluorescence emission spectra of pH-s-1. (e) Fluorescence emission spectra of pH-s+1. (Ex = 525 nm; Em = 540 nm–750 nm)



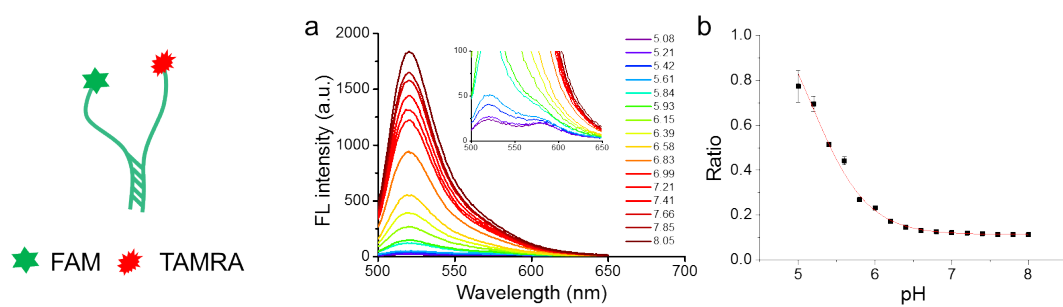


**Figure S4.** Fluorescence emission spectra (a) and the ratios curve (b) of the FAM and TAMRA dual-labelled pH-s in the buffer with indicated pH values ( $n = 3$ ). (pH-s was constructed by using the strand No. 15 and 16)

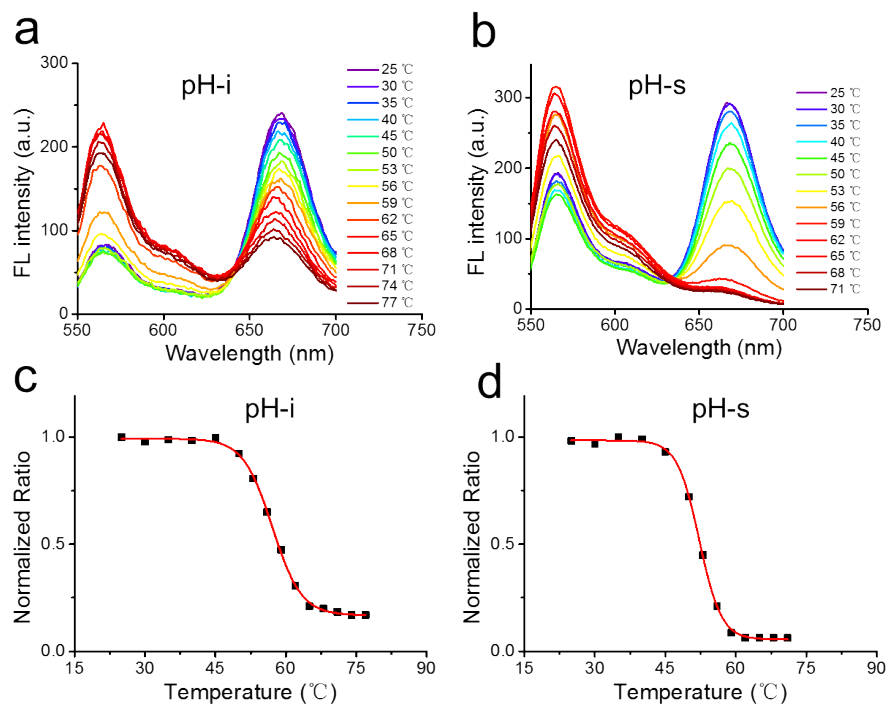


**Figure S5.** Fluorescence spectra (a, b) and normalized ratio plots (c, d) of the pH-i and pH-s in the fluorescence melting experiments at pH 5.5.

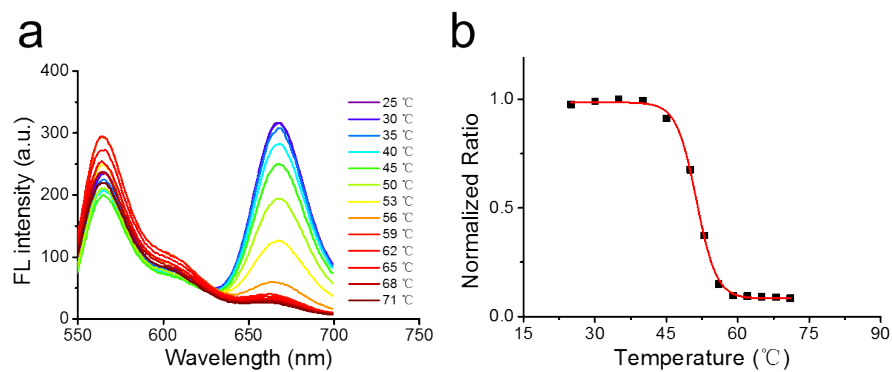


**Figure S6.** Fluorescence spectra (a) and normalized ratio plots (b) in the fluorescence melting experiments of pH-Td at pH 5.5.

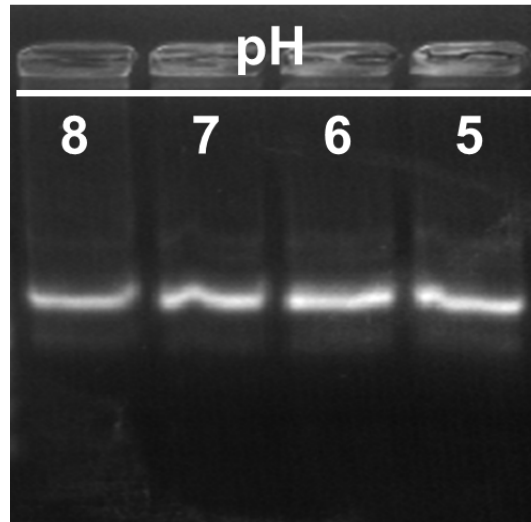


**Figure S7.** Agarose gel electrophoresis image to confirm the structural stability of the pH-Td in different pH.

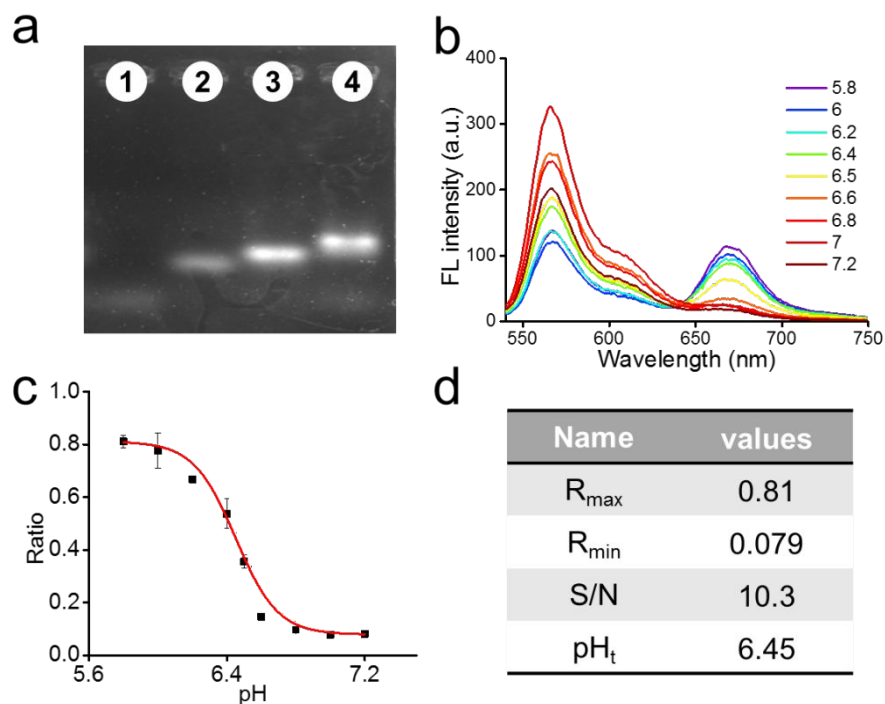


**Figure S8.** Agarose analysis and FRET-response properties of pH-Td7nt in pH sensing. (a) Agarose electrophoresis image of the step-by-step assembly of pH-Td7nt: lane 1, 7L1; lane 2, 7L1 + 7L4; lane 3, 7L1 + 7L2-5A + 7L4; lane 4, 7L1 + 7L2-5A + 7L3-3A + 7L4. (b) Fluorescence emission spectra of pH-Td7nt at different pH values (Ex = 525 nm; Em = 540 nm–750 nm). (c) The plot of fluorescence ratios of pH-Td7nt versus the pH conditions (n = 3). (d) The summary of  $R_{\max}$ ,  $R_{\min}$ , S/N and  $pH_t$  results of pH-Td7nt in the pH sensing.

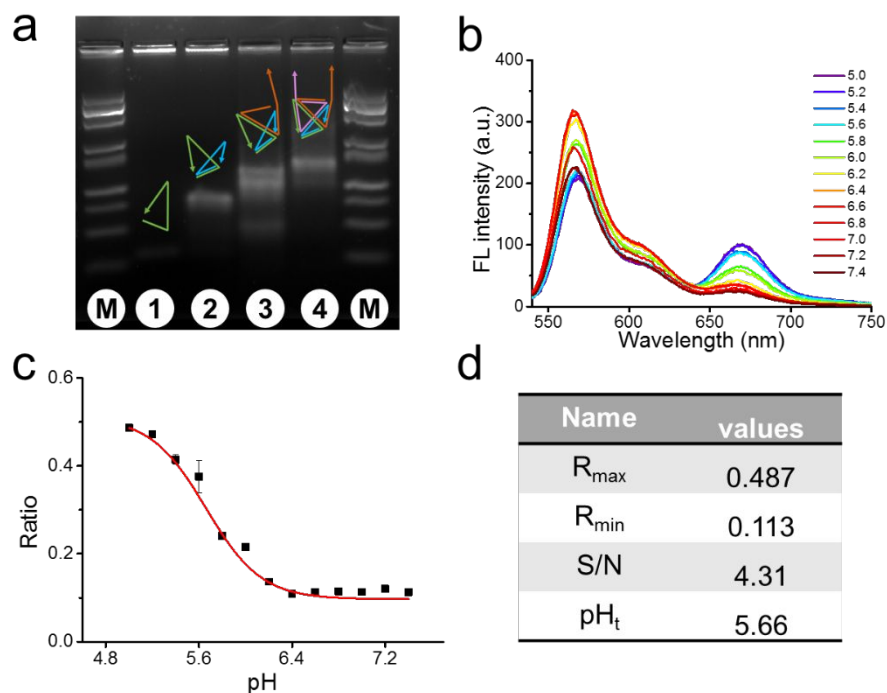


**Figure S9.** Agarose analysis and FRET-response properties of pH-Td-1 in pH sensing. (a) Agarose electrophoresis results of the step-by-step assembly of pH-Td-1: M, 25 bp DNA marker; lane 1, L1; lane 2, L1 + L4; lane 3, L1 + L2-5A-1 + L4; lane 4, L1 + L2-5A-1 + L3-3A-1 + L4. (b) Fluorescence emission spectra of pH-Td-1 at different pH values (Ex = 525 nm; Em = 540 nm–750 nm). (c) The plot of fluorescence ratios of pH-Td-1 versus pH changes (n = 3). (d) The summary of  $R_{\max}$ ,  $R_{\min}$ , S/N and  $pH_t$  results of pH-Td-1 in the pH sensing.

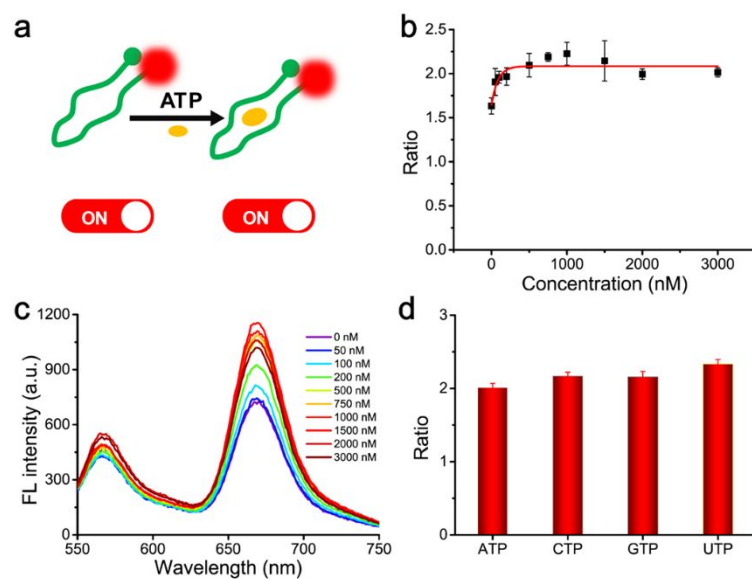


**Figure S10.** Application of the i-motif split design (ATP-i) in the sensing of ATP. (a) Conformational change of the ATP-i in the ATP sensing. (b) Fluorescence ratios and (c) spectra of the ATP-i versus ATP concentrations. (d) Specificity of the ATP sensing by the ATP-i (n = 3).

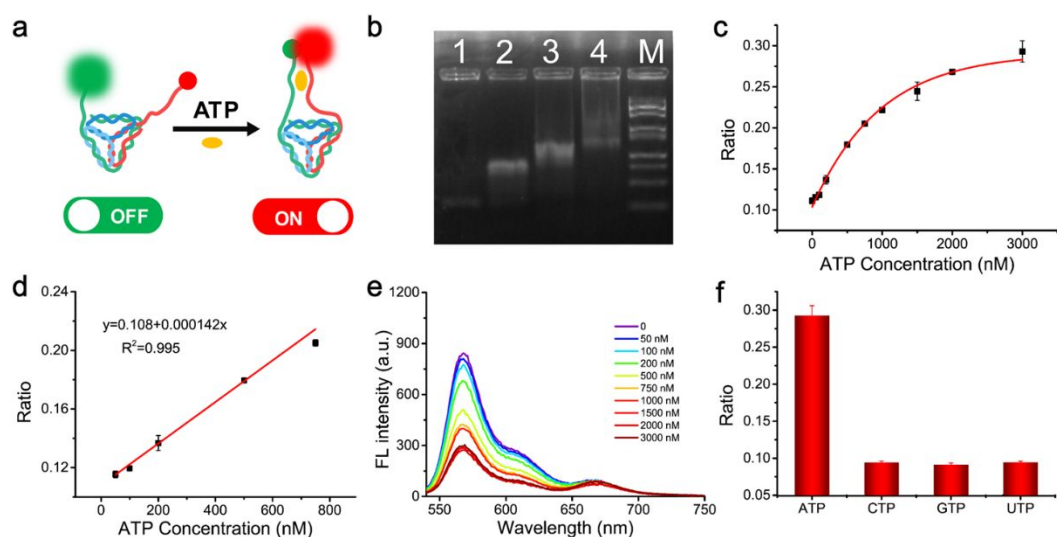


**Figure S11.** Application of the i-motif split in the Td (ATP-Td) in the sensing of ATP. (a) Conformational change of ATP-Td for the ATP sensing. (b) Agarose electrophoresis of the step-by-step assembly of the ATP-Td. (c-e) FRET response of the ATP-Td versus ATP concentrations. (f) Specificity of the ATP sensing by the ATP-Td (n = 3).



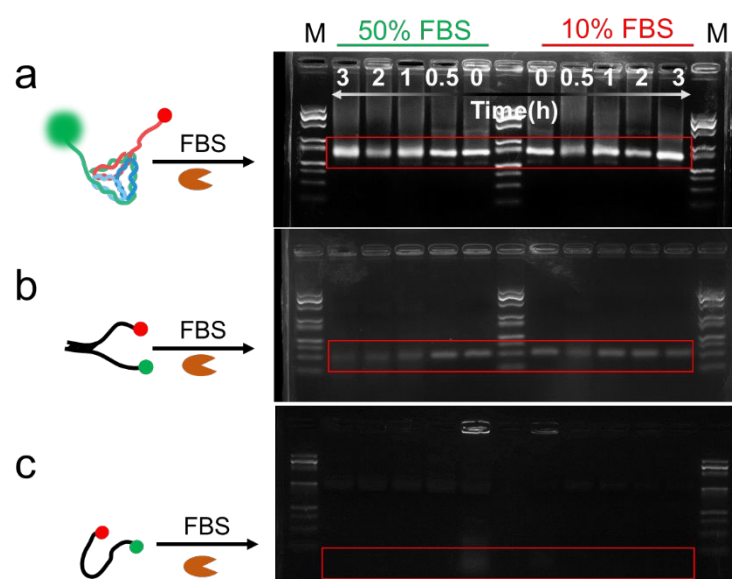


**Figure S12.** Structural stability evaluation by agarose electrophoresis analysis of pH-Td (a), pH-s (b) and pH-i (c) in 10% and 50% FBS at 37°C for different time. The red rectangle indicated the position of the corresponding band.

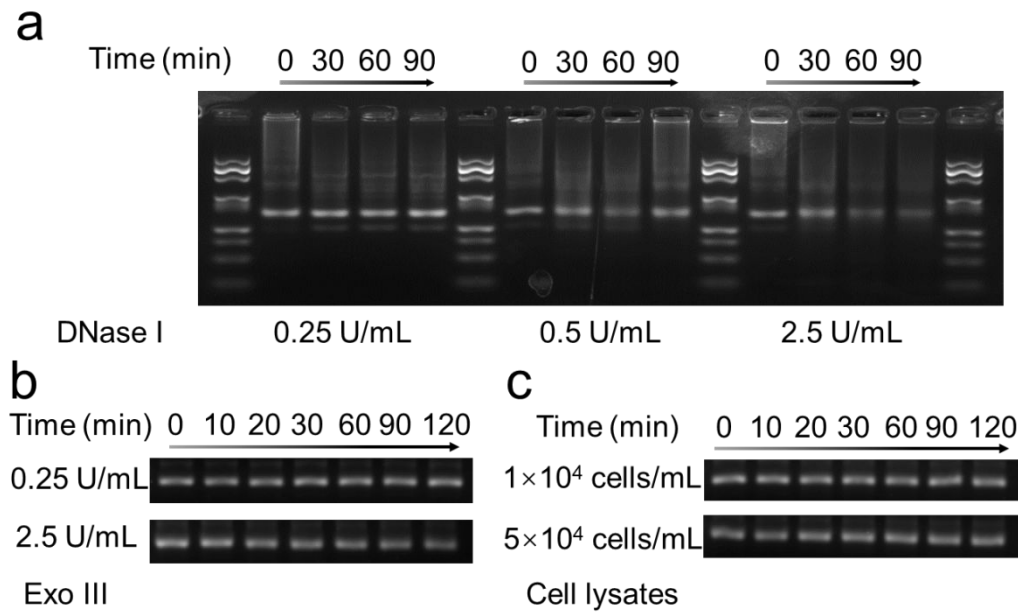


**Figure S13.** Biostability analysis of pH-Td in nucleases and cell lysates. (a) The agarose electrophoresis image of pH-Td incubated in DNase I (0.25 U/mL, 0.5 U/mL, 2.5 U/mL) for different time. (b) The agarose electrophoresis image of pH-Td incubated in Exo III (0.25 U/mL and 2.5 U/mL). (c) The agarose electrophoresis image of pH-Td incubated in cell lysates for different time.

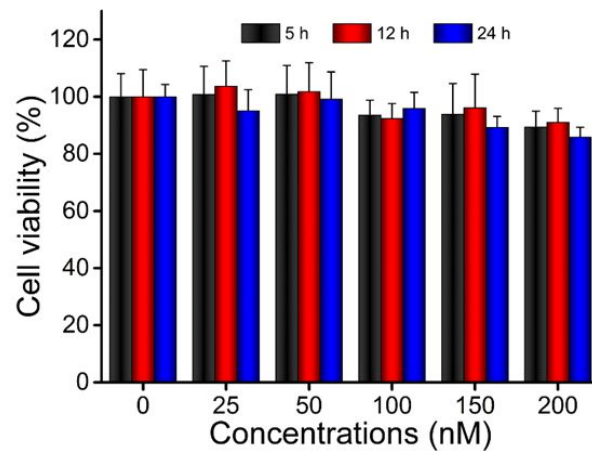


**Figure S14.** The viability experiment of NIH 3T3 cells against pH-Td (n = 6).

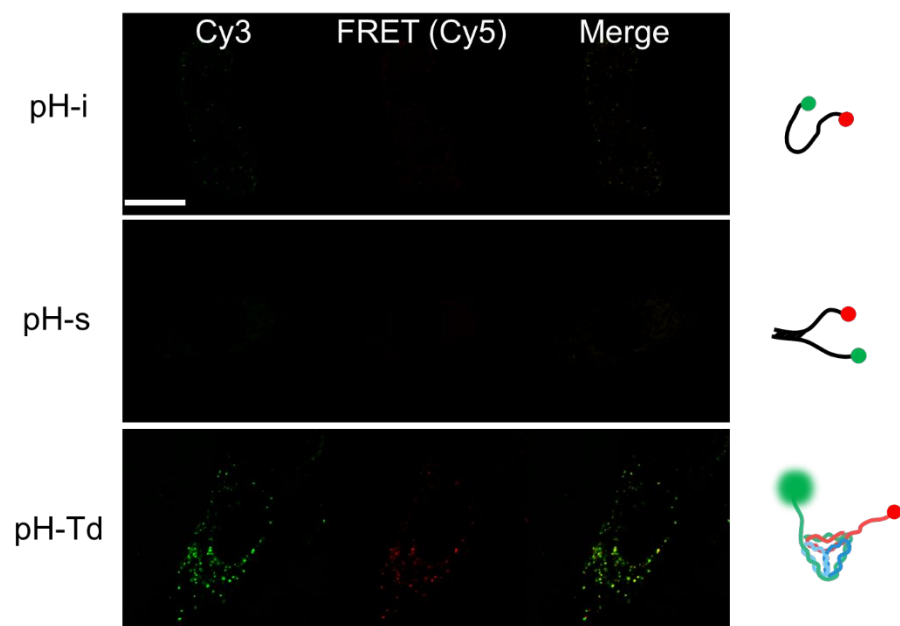


**Figure S15.** Intracellular imaging analysis of pH-i, pH-s and pH-Td. Scale bar: 10  $\mu\text{m}$ .

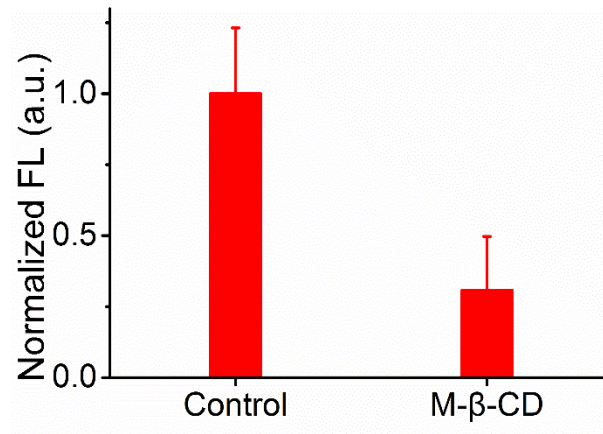


**Figure S16.** Demonstration of receptor-mediated internalization of the pH-Td in NIH 3T3 cells pretreated with 10 mM M-β-CD.

**Table S3. Comparison of i-motif-based FRET sensors for lysosomal pH imaging**

Structure of sensor	Working range	Sensitivity (S/N)	Tunable ability of pH response	Validated stability	Ref.
Tetrahedral DNA pH sensor (pH-Td)	5.4-6.8	~10	<ul style="list-style-type: none"> <li>• Yes (<math>pH_t^a</math> from 5.71 to 6.81)</li> <li>• By controlling the split sequence distance and altering the pH responsive sequence</li> </ul>	<ul style="list-style-type: none"> <li>• In DNase I (0.5 U/mL) for 1.5 h</li> <li>• In Exo III (2.5 U/mL) and cell lysates (<math>5 \times 10^4</math> cells/mL) for 2 h</li> <li>• In 50% FBS for 3 h</li> </ul>	This work
DNA triangular prism nanomachine (TPN)	5.0-7.5	~3	N/A <sup>b</sup>	<ul style="list-style-type: none"> <li>• In DNase I (0.25 U/mL) for 1 h</li> <li>• In 10% FBS and cell lysates (<math>2 \times 10^4</math> cells mL<sup>-1</sup>) for 6 h</li> </ul>	1
dsDNA pH sensor (ChloropHore)	5.5-6.5	5.5	<ul style="list-style-type: none"> <li>• Yes</li> <li>• By modifying the C-rich region with 5'-bromocytosines</li> </ul>	N/A	2
Spherical nucleic acids	5.4-7.0	~4	<ul style="list-style-type: none"> <li>• Yes</li> <li>• By tuning the mismatched based number</li> </ul>	N/A	3
dsDNA pH sensor (I-switch/I <sup>4</sup> )	5.0-7.0	~4	<ul style="list-style-type: none"> <li>• Yes (<math>pH_t</math> from 6.3 to 7.3)</li> <li>• By altering the pH responsive sequence.</li> </ul>	N/A	4
dsDNA pH sensor (I-switch)	5.5-7.0	~5.5	N/A	N/A	5

<sup>a</sup>  $pH_t$  means the pH transition midpoint.

<sup>b</sup> N/A means not available.

## Reference

- [1] Zhou, Y. J.; Wan, Y. H.; Nie, C. P.; Zhang, J.; Chen, T. T.; Chu, X. *Anal. Chem.* **2019**, *91*, 10366-10370.
- [2] Leung, K.; Chakraborty, K.; Saminathan, A.; Krishnan, Y. *Nature Nanotechnology* **2019**, *14*, 176-183.
- [3] Huang, J.; Ying, L.; Yang, X.; Yang, Y.; Quan, K.; Wang, H.; Xie, N.; Ou, M.; Zhou, Q.; Wang, K. *Anal. Chem.* **2015**, *87*, 8724-8731.
- [4] Modi, S.; Halder, S.; Nizak, C.; Krishnan, Y. *Nanoscale* **2014**, *6*, 1144-1152.
- [5] Modi, S.; M. G, S.; Goswami, D.; Gupta, G. D.; Mayor, S.; Krishnan, Y. *Nature Nanotechnology* **2009**, *4*, 325-330.